



Cite this: *Green Chem.*, 2019, **21**, 6103

Production of 3-hydroxypropionate using a novel malonyl-CoA-mediated biosynthetic pathway in genetically engineered *E. coli* strain†

Bo Liang,^{‡a,b} Guannan Sun,^{‡a,b} Zhaobao Wang,^{a,b} Jian Xiao ^c and Jianming Yang ^{*a,b}

3-Hydroxypropionic acid (3-HP) is a promising platform chemical with a wide range of applications. The traditional chemical synthesis of 3-HP is well-established, but the resource limitations, high price and toxicity of the used raw materials do not meet the new sustainable development goals. Accordingly, the microbial synthesis of 3-HP by fermentation will become a promising and attractive route mainly due to its environmentally friendly production, use of renewable resources, and sustainable development. Herein, to biosynthesize 3-HP directly from malonate, a novel malonyl-CoA-mediated biosynthetic pathway was successfully developed as follows. Firstly, various transporters involved in malonate transportation was systematically investigated and screened. Secondly, to biosynthesize 3-HP, an original strategy was employed by heterologously co-expressing the mutant of malonyl-CoA reductase (MCR) from *Chloroflexus aurantiacus* and malonyl-CoA synthetase (MatB) from *Rhodospseudomonas palustris* in the *Escherichia coli* C43 (DE3) strain, which was screened from three different MatB enzymes. Finally, to further enhance the production of 3-HP, native transhydrogenase (PntAB) and NAD kinase (YfjB) genes were expressed to increase the NADPH supply in *E. coli*. The final genetically modified strain SGN78 showed a significant improvement in malonate utilization and produced 1.20 ± 0.08 g L⁻¹ of 3-HP in the flask culture. Thus, this work demonstrates the production of 3-HP in *E. coli* with the shortest route for the biosynthesis of 3-HP, which involved only three steps from the substrate. Also, it opens a path for the biosynthesis of 3-HP and other malonyl-CoA-based valuable chemicals directly from malonate in *E. coli*.

Received 6th July 2019,
Accepted 2nd October 2019
DOI: 10.1039/c9gc02286d

rsc.li/greenchem

1. Introduction

3-Hydroxypropionic acid (3-HP) is an important platform compound, which is ranked in the list of the top 12 most potential chemicals by the US Department of Energy due to its excellent performance and broad application prospect.^{1,2} Traditionally, 3-HP can be derived from the hydrolysis of β -propiolactone or 3-hydroxypropionitrile. However, the major disadvantages of these routes are the high toxicity of the synthesis process.^{3,4} The 3-hydroxypropionitrile route needs the toxic and noxious

sodium cyanide. For the β -propiolactone route, the raw materials ketene and methanol are highly toxic, and the intermediate β -propiolactone is carcinogenic. In addition, 3-HP can also be produced directly *via* the oxidation of acrylic acid or PDO.^{3,5} However, due to the rapid increase in the price of acrylic acid and PDO in recent years, they have become economically unfavorable.³ Thus, the traditional chemical synthesis of 3-HP is well-established, but the resource limitations, high price and toxicity of the used raw materials do not meet the new sustainable development goals.⁶ Thus, compared with conventional chemical synthesis, the microbial synthesis of 3-HP by fermentation will become a promising and attractive route mainly for its many advantages, including cheaper substrates, nontoxic raw materials, mild reaction conditions and simple operation, which are compatible with sustainable development, and the reduced amounts of byproducts help reduce the cost of production.

Currently, the fermentation of 3-HP mainly focuses on various organisms using glucose and glycerol as substrates, including *Escherichia coli*,^{7–9} yeast,^{6,10,11} *Klebsiella* sp.^{12,13} *Corynebacterium glutamicum*,¹⁴ *Synechococcus* sp.^{15,16} and

^aEnergy-rich Compounds Production by Photosynthetic Carbon Fixation Research Center of Qingdao Agricultural University, People's Republic of China.
E-mail: yjming888@126.com

^bShandong Key Lab of Applied Mycology, College of Life Sciences, Qingdao Agricultural University, Qingdao, Shandong Province, People's Republic of China

^cCollege of Chemistry and Pharmaceutical Sciences, Qingdao Agricultural University, Qingdao, Shandong Province, People's Republic of China

†Electronic supplementary information (ESI) available. See DOI: 10.1039/c9gc02286d

‡These authors contributed equally to this work.

Methylobacterium sp.¹⁷ To date, the malonyl-CoA pathway is generally recognized as the shortest route for the biosynthesis of 3-HP, which is composed of three modules, including the fermentation production of acetyl-CoA in cells, production of malonyl-CoA from acetyl-CoA by acetyl-CoA carboxylase (ACC) and biosynthesis of 3-HP by malonyl-CoA reductase (MCR) from malonyl-CoA. However, the key intermediate malonyl-CoA is the essential precursor for the synthesis of polyketones and fatty acids in cells,^{18,19} and a portion of acetyl-CoA enters the tricarboxylic acid cycle (TCA) for providing energy and metabolic intermediates. Thus, great efforts have been made to improve the expression level and activity of ACC, including pulling carbon into the cytosolic pool, reducing the consumption of acetyl-CoA and constructing new acetyl-CoA pathways.⁶ However, the availability of malonyl-CoA is limiting for the production of 3-HP due to the highly regulated nature of ACC.^{7,15} Therefore, it is assumed that the supply of malonyl-CoA can be enhanced by using a substrate that is not necessary for cell growth.

Despite the extensive research on malonyl-CoA production by ACC,²⁰ evidence is available in literature showing that malonyl-CoA synthetase (MatB) also has the ability to produce malonyl-CoA directly from malonic acid, largely shortening the route for the synthesis of malonyl-CoA. MatB (EC 6.2.1.14) belongs to the AMP-forming acyl-CoA synthetase protein family (PFAM 00501) (Pfam: the protein families database) and the ANL superfamily, which contains aryl-CoA synthetases, the adenylation domains of nonribosomal peptide synthetases, and firefly luciferase.²¹ MatB catalyzes the conversion of malonate and coenzyme A to malonyl-CoA with the hydrolysis of adenosine triphosphate (ATP) into AMP and PPI *via* a ping-pong mechanism. MatB exists extensively in bacteria, mammalian mitochondria and eukaryotic organisms.^{22,23} Among them, prokaryotic MatB has been widely studied, mainly originating from *Bradyrhizobium japonicum*,²⁴ *Rhizobium leguminosarum* *bv.* *Trifolii*,²⁵ *Streptomyces coelicolor*,²⁶ *Rhodopseudomonas palustris*^{27,28} and *Rhizobium japonicum*.²⁹ The physiological function of MatB is the degradation of malonic acid in organisms, which is a classic competitive inhibitor of succinate dehydrogenase (SDH), a component of the TCA cycle and complex II of the electron transport chain.²³ As a common organic acid in plant root exudate, malonic acid has been listed as one of the top 30 chemicals that can be produced from biomass by the US Department of Energy,¹ and it has been used as a building block chemical to produce diverse valuable compounds.³⁰ In recent years, the biosynthesis of fatty acids, polyketides and flavonoids from malonic acid has been realized.³¹ For example, flavonoid production was improved 7-fold through the introduction of the malonate assimilation operon into *Streptomyces venezuelae*.³² However, the utilization of malonate to produce malonyl-CoA-based valuable bio-products in *E. coli* has rarely been reported.

To date, several types of malonate transporters have been reported, including a putative malonate carrier protein (MatC) in *R. leguminosarum* *bv. trifolii*²⁵ and classified malonate/sodium symporter MdcF from *Klebsiella pneumoniae*.³³ In addition to the above transporters, tripartite ATP-independent

periplasmic (TRAP) transporters involving malonate transport have been identified in *Rhodobacter capsulatus* and *Sinorhizobium meliloti*.^{34,35} TRAP transporters are a family of substrate-binding protein (SBP)-dependent secondary transporters in prokaryotes, composed of three subunits, the substrate-binding protein (SBP), and the large and small-transmembrane domains (TMDs).³⁶ TRAP transporters are not only involved in C4-dicarboxylate transportation, but also are essential for the uptake of sialic acid and *N*-acetylneuraminic acid.³⁷ However, the ability of all the above transporters to take in exogenous malonate into *E. coli* has not been identified.

In this study, the feasibility of the production of 3-HP using malonate as the substrate was demonstrated. We expressed the malonate metabolic pathway for 3-HP production by introducing the transporters MatB and MCR into *E. coli*. We observed malonate transport and the production of 3-HP directly from malonate (Fig. 1). Finally, our resultant strain accumulated 1.20 ± 0.08 g L⁻¹ 3-HP using glucose as the sole carbon source and malonate as the substrate in shaking flask cultivation. These results demonstrate the *in vivo* functioning of the metabolic pathway composed of the malonate transporters MatB and MCR, and the effect of carbon flux enhancement by bypassing ACC. To the best of our knowledge, this is the first report of a technique for the efficient production of the plat-

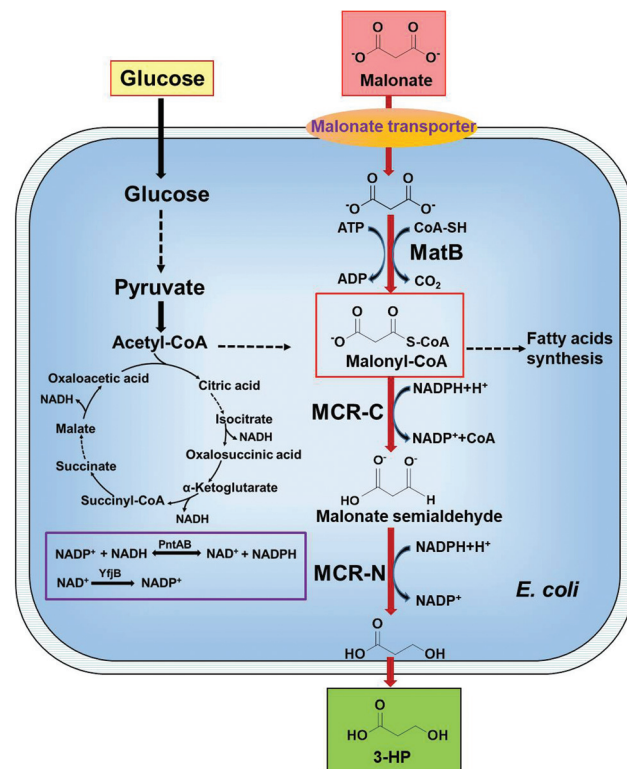


Fig. 1 3-HP synthetic pathway in *E. coli* using malonate as the substrate. The pathway used in herein is noted by red arrows. MatB: malonyl-CoA synthetase; MCR: malonyl-CoA reductase; PntAB: transhydrogenase; and Yjfb: NAD kinase. The expression of multiple genes was conducted using plasmids and chromosomal integration.

form chemical 3-HP from malonate. This novel malonyl-CoA-mediated biosynthetic pathway can realize the shortest route for the bioproduction of 3-HP, which is characterized by easy-to-control process, cost-effectiveness and low by-products, providing an attractive and eco-friendly substitute over the existing chemical synthetic routes.

2. Materials and methods

2.1 Bacterial strains and growth conditions

All PCR primers for gene amplification and strains used in this study are listed in Tables S1 and S2.† *E. coli* DH5 α was used for recombinant DNA manipulation, while *E. coli* C43 (DE3) was the host for the expression of enzymes. *E. coli* strains were grown in Luria-Bertani (LB) medium at 37 °C with shaking. For 3-HP production, the different strains were cultivated in shake-flask conditions with medium containing 20 g L⁻¹ glucose, 4.5 g L⁻¹ K₂HPO₄·3H₂O, 9.0 g L⁻¹ (NH₄)₂SO₄, 3.0 g L⁻¹ citric acid monohydrate, 3.0 g L⁻¹ trisodium citrate, 5.7 g L⁻¹ KCl, 0.226 g L⁻¹ FeSO₄·7H₂O, 0.5 g L⁻¹ MgSO₄, and 0.1 mL trace element solution, which included (NH₄)₆Mo₇O₂₄·4H₂O 3.7 g L⁻¹, ZnSO₄·7H₂O 2.9 g L⁻¹, H₃BO₃ 24.7 g L⁻¹, CuSO₄·5H₂O 2.5 g L⁻¹, and MnCl₂·4H₂O 15.8 g L⁻¹. Where appropriate, antibiotics were added as follows: ampicillin (Amp, 100 μ g mL⁻¹), kanamycin (Kan, 50 μ g mL⁻¹) and chloramphenicol (Cm, 34 μ g mL⁻¹).

2.2 Construction of plasmids

2.2.1 Construction of plasmids for expressing malonate transporters. The genes encoding MatC from *R. leguminosarum* *bv trifolii* (GenBank No. ACI53872.1), MdcF from *K. pneumoniae* (GenBank No. AAC45458.1), TRAP dicarboxylate transporter from *S. meliloti* (consisting of DctM, DctQ and DctP subunits, responding to GenBank No. ABR63913.1, AAK64740.1 and ABR63911.1, respectively) (namely MatPQM) and TRAP dicarboxylate transporter from *R. capsulatus* (consisting of DctM, DctQ and DctP subunits, responding to GenBank No. CAA45387.1, CAA45386.1 and CAA45385.1, respectively) (namely DctPQM) were codon-optimized for *E. coli* and synthesized by Genaray Biotech Co., Ltd (Shanghai, China). MatC, MdcF, MatPQM and DctPQM encoding genes were amplified from cloning vector by PCR using primers matC-F/matC-R, mdcF-F/mdcF-R, matPQM-F/matPQM-R and dctPQM-F/dctPQM-R, respectively, and separately inserted into the *Bam*H I/*Hind* III sites of pET-28a(+) to generate plasmids pSGN-10 (pET28-matC), pSGN-18 (pET28-mdcF), pSGN-20 (pET28-matPQM), pSGN-21 (pET28-dctPQM), respectively. To construct plasmids pSGN-69 (pBAD24-matC), pSGN-70 (pBAD24-mdcF), pSGN-68 (pBAD24-matPQM) and pSGN-72 (pBAD24-dctPQM), all the above genes were amplified by PCR using primers matC-F1/matC-R1, mdcF-F1/mdcF-R1, matPQM-F1/matPQM-R1 and dctPQM-F1/dctPQM-R1 respectively, and separately cloned into the *Pst* I sites of pBAD24 using the ClonExpress Ultra One Step Cloning Kit (Vazyme Biotech Co., Ltd, China). For the obtained vectors pSGN-22 (pMAL-c2x-matC), pSGN-25 (pMAL-c2x-mdcF),

pSGN-27 (pMAL-c2x-matPQM) and pSGN-28 (pMAL-c2x-dctPQM), all the above genes were amplified by PCR using primers matC-F/matC-R2, mdcF-F/mdcF-R2, matPQM-F/matPQM-R2 and dctPQM-F/dctPQM-R2, respectively, and separately cloned into the *Bam*H I/*Sal* I sites of pMAL-c2x.

2.2.2 Construction of plasmids expressing MatB. Three genes encoding MatB from *R. palustris* (GenBank No. CAE25665.1) (namely *Rp*MatB), *B. japonicum* (GenBank No. AAF28840.1) (namely *Bj*MatB) and *Arabidopsis thaliana* (GenBank No. OAP02278.1) (namely *At*MatB) were synthesized by Genaray Biotech Co., Ltd (Shanghai, China) with codon optimization for *E. coli*. These three MatB genes were amplified from cloning vector by PCR using primers *Rp*matB-F/*Rp*matB-R, *Bj*matB-F/*Bj*matB-R and *At*matB-F/*At*matB-R, and inserted into the *Bam*H I and *Hind* III sites of pACYCDuet-1 to generate plasmids pSGN-01 (pACYCDuet-*Rp*matB), pSGN-15 (pACYCDuet-*Bj*matB) and pSGN-16 (pACYCDuet-*At*matB), respectively.

2.2.3 Construction of plasmids for co-expressing MatB and MCR. Two types of genes encoding the MCR mutant N940V/K1106W/S1114R were synthesized from Genaray Biotech Co., Ltd (Shanghai, China), including MCR with a linker (GGGGS) between the N-terminal domain and C-terminal domain and MCR without any redundant amino acid between the N-terminal domain and C-terminal domain. To generate plasmid pSGN-34 (pRSFDuet-mcr) and pSGN-35 (pRSFDuet-mcr(linker)), the MCR encoding genes were amplified from cloning vector by PCR using primers mcr-F1/mcr-R1, and inserted into the *Bgl* II and *Xho* I sites of pRSFDuet-1. Then the *Rp*matB encoding gene was amplified from cloning vector by PCR using primers matB-F1/matB-R1, and inserted into the *Bam*H I site of the above plasmids to generate pSGN-40 (pRSFDuet-*Rp*matB-mcr) and pSGN-41 (pRSFDuet-*Rp*matB-mcr(linker)). The plasmid pSGN-36 (pRSFDuet-mcr(linker)-*Rp*matB) was constructed by cloning the MCR encoding gene into the *Bam*H I and *Sal* I sites of pRSFDuet-1 with primers mcr-F2/mcr-R2 and then cloning *Rp*matB into the *Bgl* II site with primers matB-F2/matB-R2.

2.2.4 Construction of plasmids expressing PntAB. The gene encoding PntAB was amplified from the *E. coli* DH5 α genome by PCR using primers pntAB-F/pntAB-R, and then the PntAB gene was inserted into the *Hind* III site of pSGN-41 (pRSFDuet-*Rp*matB-mcr(linker)) to generate plasmid pSGN-42 (pRSFDuet-*Rp*matB-PntAB-mcr(linker)) using the ClonExpress Ultra One Step Cloning Kit (Vazyme Biotech Co., Ltd, China).

2.2.5 Chromosomal integration of YfjB gene. The integration was carried out using suicide vector pRE112.⁷ The yfjB gene was cloned from *E. coli* DH5 α by PCR with primers yfjB-F/yfjB-R. The promoter of glyceraldehyde phosphate dehydrogenase (*P*_{gapdh}) and yfjB gene was inserted into the *Pst*I sites of pRE112- Δ prpR to generate the plasmid pRE112-yfjB, which was used to mediate the allelic exchange to generate SGN34.

2.3 Identification of malonate transportation function in *E. coli*

E. coli C43 (DE3), SGN10, SGN18, SGN20, SGN21, SGN22, SGN25, SGN27, SGN28, SGN68, SGN69, SGN70 and SGN72

strains were separately cultured in 100 mL LB/IPTG or arabinose/malonate medium with Kan or Amp at 30 °C for enzyme production and malonate transportation. After 16 h shaking, the cell cultures were collected for the following experiments.

2.3.1 Transcription analysis of transporter genes. A portion of the collected cells was disrupted by lysozyme. Total RNA was isolated using the TRIzol reagent method (Takara Company, Japan). The RNA concentration was quantified using a NanoDrop ND1000 (Thermo Scientific, Wilmington, DE, USA). Transporter encoding gene expression analysis was performed using quantitative reverse transcription PCR (qRT-PCR). 16S rRNA was used as the internal standard.³⁸ The primers used for the assays are indicated in Table S3.† The cDNA synthesis kit was used for reverse transcription (Takara Company, Japan). ChamQ Universal SYBR qPCR Master Mix (Vazyme Biotech Co., Ltd, China) and qTOWER³ Real-Time PCR Thermal Cycler (Jena, Germany) were used for all quantitative assays. The comparative C_T method was used for relative quantification of gene expression. The relative quantification for each of the mRNA levels was calculated using the ΔC_T method, which is the difference between the C_T of the gene of interest and that of the reference gene.

2.3.2 Protein expression analysis of transporter genes. Another portion of collected cells was disrupted by sonication, and the crude extracts were centrifuged, and the supernatants were used for western blot analysis. Protein samples were electroblotted onto PVDF membrane and allowed to incubate with Anti-His Tag Mouse Monoclonal Antibody (Solarbio, China). Subsequently, the samples were probed with Antimouse IgG secondary antibody conjugated with HRP. After washing with PBST, BCIP/DAB (Solarbio, China) was added to detect antigen-antibody conjugates. The reaction was quenched with distilled water.

2.3.3 Malonate transportation function analysis of transporter genes in *E. coli*. The concentration of malonate in the supernatants of the cell cultures was detected by HPLC with Sepax Carbomix H-NP10 column (300 mm × 7.8 mm, 10 μm). The mobile phase was 2.5 mM H₂SO₄, and the flow rate was 0.6 mL min⁻¹ at a temperature of 55 °C. The amount of malonate was detected by a UV detector with a wavelength of 210 nm.

2.4 Protein purification and determination of kinetic parameters of MatB

SGN01, SGN15 and SGN16 were separately cultured in LB/Cm/IPTG medium at 20 °C for enzyme production. After 16 h shaking, the cells were disrupted by sonication, and the supernatants were collected by centrifugation (13 000 rpm, 40 min) at 4 °C. The sample was loaded onto an Ni-NTA column pre-equilibrated with resuspended buffer (20 mM PBS pH 7.4, 300 mM NaCl). Then the column was washed with washing buffer (20 mM PBS pH 7.4, 300 mM NaCl, 15 mM imidazole, and 1 mM β-mercaptoethanol). The bound protein was eluted with elution buffer (20 mM PBS pH 7.4, 300 mM NaCl, 300 mM imidazole, and 1 mM β-mercaptoethanol). Finally, the protein was dialyzed, concentrated and stored at -80 °C.

Protein purity was analyzed by SDS-PAGE, and protein concentration was determined *via* the Bradford assay.

For the determination of kinetic parameters, the purified enzyme was incubated with various concentrations of malonate ranging from 40 to 1200 μM at 37 °C. The assay mixture contained 100 mM K₃PO₄ buffer (pH 7.0), 0.2 mM CoA, 0.4 mM ATP, and 2 mM MgCl₂. The concentration of purified enzyme was 0.052 μM for *RpMatB*, 0.104 μM for *BjMatB* and 0.087 μM for *AtMatB*. The reaction was stopped by adding an equal volume of methanol. The concentrations of malonyl-CoA were determined by HPLC with a ThermoFisher Ultimate 3000 using a C18 column (250 mm × 4.6 mm, 5 μm). The mobile phase consisted of solvent A (100 mM potassium phosphate, pH = 5.2) and solvent B (acetonitrile). The gradient elution procedure was as follows: 0 to 5 min, 1.2% of B; 5 to 45 min, and a linear gradient from 1.2% to 12% of B. The flow rate was 0.5 mL min⁻¹ at a temperature of 25 °C. The amount of malonyl-CoA was detected by a UV detector with a wavelength of 245 nm.³⁹ The kinetic constants were calculated by fitting the initial rate data into the Michaelis-Menten equation using the Graph-Pad Prism 5 software (GraphPad Software, Inc., USA, <http://www.graphpad.com>).

2.5 Synthesis of 3-HP using malonate as substrate

Plasmids pSGN-36(pRSFDuet-mcr(linker)-*RpmatB*), pSGN-40(pRSFDuet-*RpmatB*-mcr) and pSGN-41(pRSFDuet-*RpmatB*-mcr(linker)) were separately co-transformed with pSGN-68(pBAD24-matPQM) in *E. coli* C43 (DE3) to generate strains SGN73, SGN74 and SGN75, respectively. Plasmids pSGN-42(pRSFDuet-*RpmatB*-pntAB-mcr(linker)) and pSGN-68(pBAD24-matPQM) were co-transformed into *E. coli* C43 (DE3):*yfjB* to make strain SGN78. The strains were grown in fermentation medium, as described above, supplemented with ampicillin (100 μg mL⁻¹) and kanamycin (30 μg mL⁻¹) at 200 rpm and 37 °C to an optical density at 600 nm (OD₆₀₀) value of 0.6, and then induced with IPTG (final concentration of 0.6 mM) as well as arabinose (final concentration of 0.1%) at 30 °C for 16 h. Simultaneously, substrate malonate was added to the culture to synthesize 3-HP. The supernatants obtained by the centrifugation of the culture samples at 10 000g for 10 min were filtered through a 0.22 μm filter and eluted through a C18 column (250 mm × 4.6 mm, 5 μm) with methanol-10 mM H₃PO₄ (5 : 95, v/v) as the mobile phase. The flow rate and the detection wavelength were set to 1.5 mL min⁻¹ and UV 210 nm, respectively.⁹ The product was characterized by direct comparison with standard 3-HP (Sigma-Aldrich, USA). The peak area was converted to 3-HP concentration by comparison with a standard curve plotted with a set of known concentration of 3-HP.

2.6 Optimization of fermentation process

2.6.1 Effect of organic nitrogen source. The shake-flask cultures were incubated in different organic nitrogen sources (BE (So), beef extract from Solarbio; BE(Si), beef extract from Sinopharm; T, tryptone; and YE, yeast extract) at 20 °C for 16 h with the concentration of IPTG and arabinose of 0.5 mM and

0.2%, respectively. Simultaneously, the substrate malonate was added to the culture to synthesize 3-HP, and the 3-HP products were calculated.

2.6.2 Effect of induction temperature. The *E. coli* strain was inoculated in 50 mL of fermentation medium with the most suitable organic nitrogen source and cultured at 37 °C with shaking at 180 rpm. When the OD₆₀₀ of the bacterial culture reached 0.6, the shake-flask cultures were incubated at different induction temperatures (16 °C, 20 °C, 30 °C, 34 °C and 37 °C) for 16 h with the concentration of IPTG and arabinose of 0.5 mM and 0.2%, respectively. Simultaneously, the substrate malonate was added to the culture to synthesize 3-HP, and the 3-HP products were assayed.

2.6.3 Effect of inducer (IPTG and arabinose) concentration. The shake-flask culture was incubated in different inducer (IPTG) concentrations (0.1 mM, 0.25 mM, 0.5 mM and 1 mM) and inducer (arabinose) concentrations (0.05%, 0.1%, 0.2%, 0.3% and 0.4%) at the above-optimized temperature for 16 h. Simultaneously, the substrate malonate was added to the culture to synthesize 3-HP, and the 3-HP products were measured.

2.6.4 Effect of liquid volume. The *E. coli* strain was cultured in 250 mL shake-flasks with different liquid volumes (30 mL, 50 mL, 80 mL, 100 mL, and 120 mL) at 37 °C and 180 rpm. When the OD₆₀₀ of the bacterial culture reached 0.6, the shake-flask cultures were incubated at 30 °C for 16 h with the concentration of IPTG and arabinose of 0.6 mM and 0.1%, respectively. Simultaneously, the substrate malonate was added to the culture to synthesize 3-HP, and the 3-HP products were detected.

2.6.5 Effect of induction opportunity. The *E. coli* strain harboring expression vectors were grown to an optical density at 600 nm (OD₆₀₀) value of 0.4–1.0, and then induced with IPTG (0.6 mM) and arabinose (0.1%) at 30 °C for 16 h. Simultaneously, the substrate malonate was added to the culture to synthesize 3-HP, and the 3-HP products were assayed.

2.6.6 Effect of induction time. *E. coli* cell-carrying expression vectors were grown at 200 rpm and 37 °C. When the culture reached an OD₆₀₀ value of 0.6, IPTG (0.6 mM) and arabinose (0.1%) were added to the culture for the induction of recombinant protein expression, and then further cultivated at 30 °C for 8 h, 12 h, 16 h, 24 h and 36 h. Simultaneously, the substrate malonate was added to the culture to synthesize 3-HP. The samples were taken regularly to determine 3-HP.

2.7 Determination of MCR and MatB activities of crude extract

SGN73, SGN74 and SGN75 were separately cultured in LB/Km/IPTG/arabinose medium at 30 °C for enzyme production. After 16 h shaking, the cells were disrupted by sonication, and the supernatants were collected by centrifugation (13 000 rpm, 40 min) at 4 °C. The reaction mixtures (0.5 mL, 37 °C) were prepared for product analysis. Each reaction contained 100 mM potassium phosphate buffer (pH 7.0), 40 mM sodium malonate, 0.2 mM CoA, 0.4 mM ATP, and 2 mM MgCl₂ and

1 mL crude extract. The incubation time for the assays for MatB activity was 30 min. The reaction was stopped by adding an equal volume of methanol. The concentrations of malonyl-CoA were determined by HPLC.

The reaction mixture for the determination of MCR activity (500 μl) contained 100 mM Tris-HCl (pH 7.8), 2 mM MgCl₂, 0.4 mM NADPH, and 1 mL (each) crude extract. The reaction was started by the addition of 0.15 mM malonyl-CoA and incubated at 37 °C for 30 min. Then the reaction was stopped by the addition of an equal volume of acetonitrile. After centrifugation, the supernatant (3-HP) was analyzed by HPLC.⁴⁰

2.8 Determination of NADPH levels

The *E. coli* SGN78 and SGN74 strains were cultured in 250 mL shake-flasks with LB/Km/IPTG/arabinose medium at 30 °C and 180 rpm. The cells with 1 mL B1 of NADPH Kit (ChemPartner, China) were broken on ice and incubated at 60 °C for 30 min. Then the supernatants were collected by centrifugation (12 000 rpm, 10 min) at 4 °C. After centrifugation, solutions I, II, and III were added and the NADPH concentration was monitored at 450 nm using an Agilent, Cary 60 Bio UV-Visible spectrophotometer.

3. Results and discussion

3.1 Transport of malonate by various malonate transporters in *E. coli*

To identify suitable malonate transporters, we screened several protein candidates. We used MatC from *R. leguminosarum* *bv trifolii*, MdcF from *K. pneumoniae*, TRAP dicarboxylate transporter from *S. meliloti* and TRAP dicarboxylate transporter from *R. capsulatus*. We examined each malonate transporter in detail by determining their transcription, expression and function in *E. coli* cells. To elucidate the function of each transporter, an appropriate set of expression vectors was constructed for the *matC*, *matPQM*, *dctPQM* and *mdcF* genes under the IPTG-inducible T7 and tac promoter, as well as the arabinose araBAD promoter (Fig. 2A and Fig. S1A†). After induction with inducers, malonate was added to the medium. After 16 h further culture at 30 °C, the cells and supernatant were separately collected.

Firstly, we assessed the expression of the target genes (Fig. 2C and Fig. S1C†). The results showed that the *matC* and *matPQM* genes were obviously transcribed in *E. coli* when three types of expression vectors were used. Varying results were obtained when different plasmids were used to express MdcF. Obvious transcription was observed only when the pBAD24 plasmid was used to express MdcF, although a slight transcription was obtained using tac promoter. Moreover, *dctPQM* failed to be transcribed in *E. coli* regardless of the plasmid used.

Then, the whole-cell crude extract was obtained and analyzed by immunoblot assay. As shown in Fig. 2B and Fig. S1B,† compared with the negative control, the strains harboring MatPQM and MatC have specific expression bands corres-

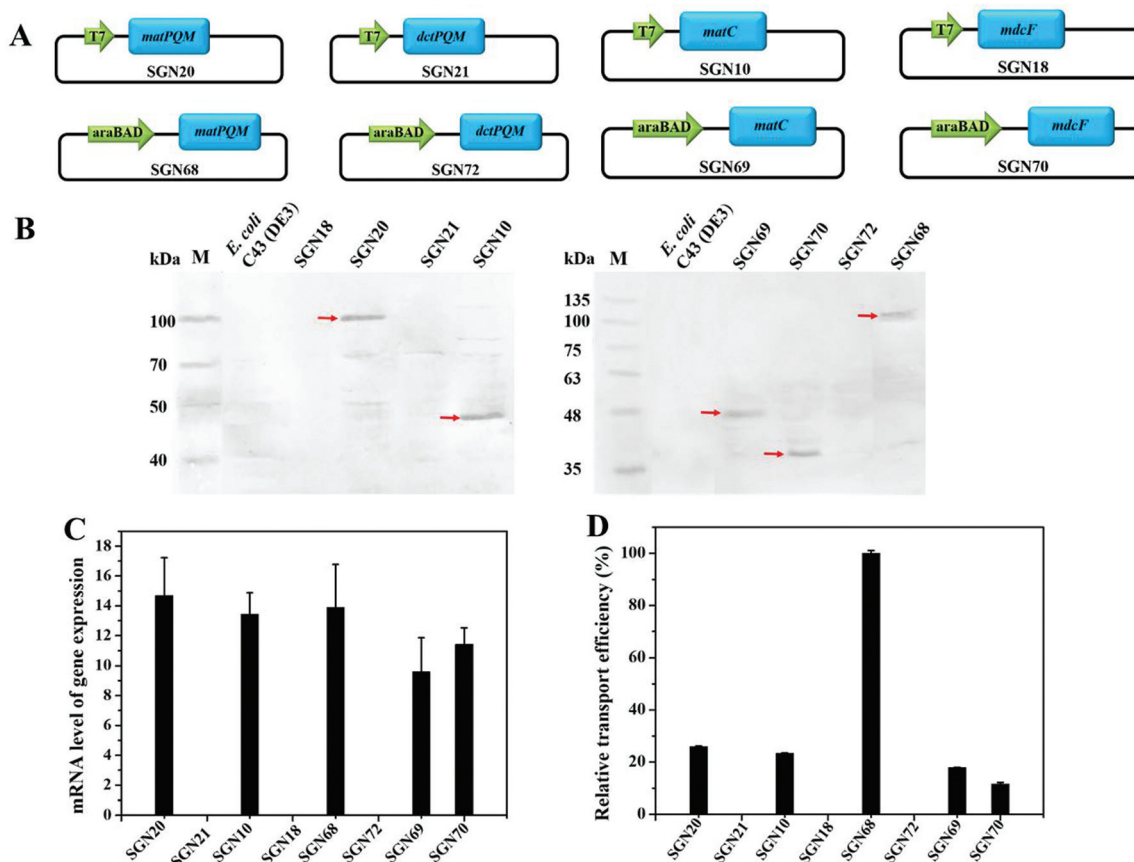


Fig. 2 Identification of malonate transportation function in *E. coli*. (A) Construction of recombinant strains carrying malonate transport genes. (B) Western blot analysis of expressed malonate transport proteins. (C) Transcription analysis of transporter genes. (D) Relative malonate transport efficiency of tested transporters.

ponding to the MatPQM and MatC protein (about 106 kDa and 46 kDa), respectively. However, there was no obvious expressed protein band in the result of the other strains even though the genes were codon-optimized and controlled by the same T7 and *tac* promoters. When these malonate transporters were expressed by arabinose inducer, besides strains SGN68 and SGN69, strain SGN70 also produced considerable proteins (40 kDa). The observed transcription of MatPQM and MatC genes under these three promoters as well as the protein expression bands suggest that these two transporters were successfully produced in *E. coli*.

To further investigate their functions, the amount of malonate in the supernatants was determined. As depicted in Fig. 2D and Fig. S1D,[†] for the TRAP system from *S. meliloti*, different expression plasmids led to obvious differences in transport activity. Especially, when pBAD24 was used as the expression vector, the transport efficiency of the recombinant strain SGN68 reached the highest level, which was about three and twenty-four times higher than that of strains SGN20 and SGN27, respectively. In contrast, MatC showed almost the same transport activity when varying the expression vector. Similar to the results from the transcription analysis, quite different activity was observed for cloning *mdcF* genes with

three types of vector. Unfortunately, the TRAP system from *R. capsulatus* has no function in *E. coli*.

A previous study suggested that the organization and arrangement of the genes involved in malonate transport vary across different rhizobia. In *R. leguminosarum* *bv. trifolii*, only the *matC* gene performs malonate transport.²⁵ However, in *S. meliloti*, the three genes (MatP, MatQ and MatM) are responsible for malonate uptake.³⁵ The amino acid residues of MatP, MatQ and MatM exhibited similarity to the DctP, DctQ and DctM subunits of the C4-dicarboxylate TRAP transporter (DctPQM) from *R. capsulatus* (24%, 25% and 31% identity), respectively.³⁵ It has been shown that the TRAP transporter uses an SBP that captures specific solutes with high affinity and transfers them to their partner permease complex located in the bacterial inner membrane.³⁶ The TRAP transporters employed by *S. meliloti* may have such a high affinity that they can acquire malonate effectively. To the best of our knowledge, this is the first detailed investigation of the transporters involved in malonate transport in *E. coli*.

3.2 Characterization of MatB

Three types of MatB were purified and analyzed by SDS-PAGE analysis (Fig. 3A). Then, the kinetic analysis of MatB for malonate

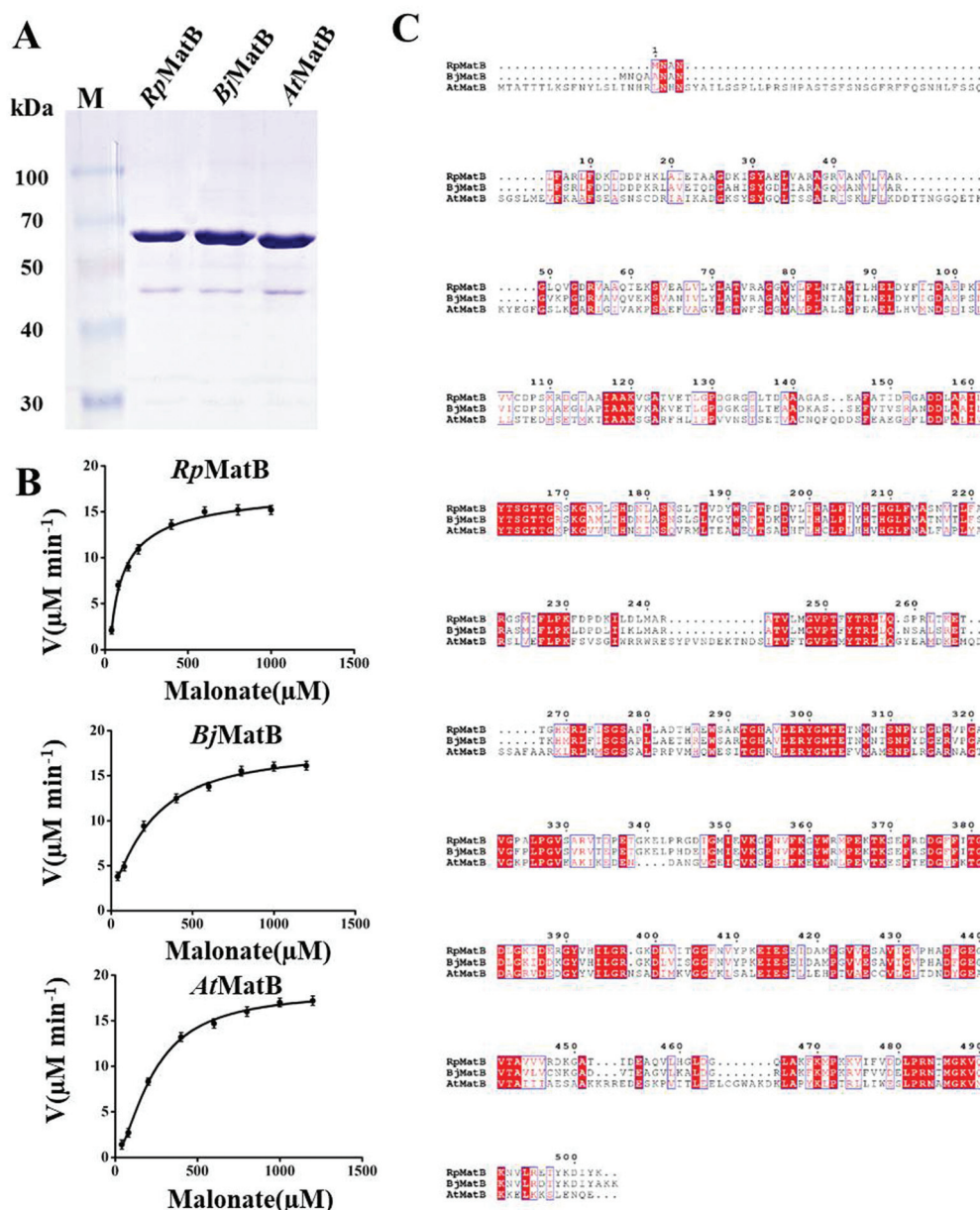


Fig. 3 Characterization of MatB. (A) SDS-PAGE analysis of the purified MatB. (B) Michaelis–Menten equation curves for three types of MatB. (C) Sequence alignment of MatB from *R. palustris* (*RpMatB*), *B. japonicum* (*BjMatB*) and *A. thaliana* (*AtMatB*). The alignment was performed using ClusterW and output was generated by ESPript.

Table 1 Kinetic analysis with malonate of MatB

Enzyme	K_M (μM)	k_{cat} (min^{-1})	k_{cat}/K_M ($\text{min}^{-1} \mu\text{M}^{-1}$)
<i>RpMatB</i>	146.8 ± 19.26	355.3 ± 13.76	2.42 ± 0.22
<i>BjMatB</i>	299.0 ± 50.52	204.4 ± 13.19	0.68 ± 0.07
<i>AtMatB</i>	386.9 ± 70.78	275.3 ± 18.67	0.71 ± 0.08

nate was performed. As shown in Fig. 3B and Table 1, the K_M value of *RpMatB* was $146.8 \pm 19.26 \mu\text{M}$, which was half of that of *BjMatB* and nearly a third of that of *AtMatB*. *RpMatB* had a k_{cat} of $355.30 \pm 13.76 \text{ min}^{-1}$. This represents a minor increase

in turnover rate (k_{cat}) over the other two types of MatB. Consequently, the k_{cat}/K_M value of *RpMatB* ($2.42 \pm 0.22 \text{ min}^{-1} \mu\text{M}^{-1}$) was 2.56- and 2.41-fold higher than that of *BjMatB* ($0.68 \pm 0.07 \text{ min}^{-1} \mu\text{M}^{-1}$) and *AtMatB* ($0.71 \pm 0.08 \text{ min}^{-1} \mu\text{M}^{-1}$), respectively. Our results were similar to that reported earlier,^{27,41} suggesting that *RpMatB* has higher affinity for malonate and higher catalyzing efficiency than the other two MatB proteins. The amino acid sequence of *RpMatB* exhibits 82% and 35% identity with *BjMatB* and *AtMatB*, respectively (Fig. 3C). Although the X-ray crystal structure of *RpMatB* has been resolved, the mechanistic basis of higher activity remains hard to understand due to the lack of *BjMatB* and *AtMatB*

protein structure information. Therefore, *RpMatB* was chosen for the synthesis of 3-HP using malonate as the substrate in our following study.

3.3 Biosynthesis of 3-HP in engineered strains

To realize the *in vivo* synthesis of 3-HP in the recombinant *E. coli* strains, the co-expression of *RpMatB* and MCR was investigated (Fig. 4A). MCR of *C. aurantiacus* is a bifunctional

enzyme with an apparent K_M value of $41.7 \pm 2.2 \mu\text{mol}$ for malonyl-CoA.⁴⁰ The N-terminal and the C-terminal region of MCR were functionally distinct. MCR-C catalyzes the reduction of malonyl-CoA to malonate semialdehyde, which can be reduced to 3-HP by MCR-N. The first step is the rate-limiting step. Thus, great efforts have been made to increase the activity of MCR-C. Some mutants with increased activity have been obtained in previous studies. Among them, the MCR

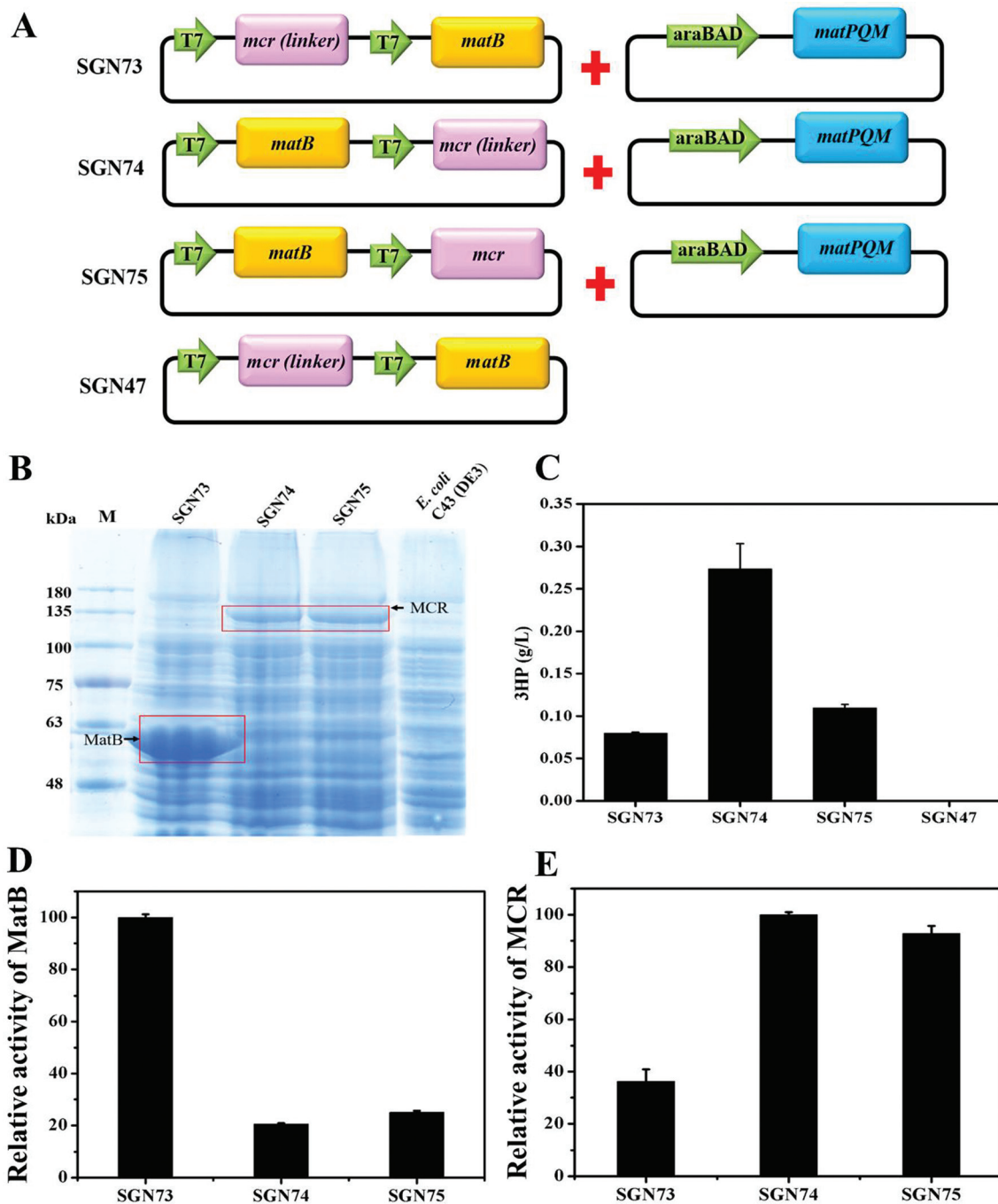


Fig. 4 Biosynthesis of 3-HP in engineered strains. (A) Construction of 3-HP biosynthesis strains. (B) SDS-PAGE analysis of crude extract of the engineered strains. (C) Biosynthesis of 3-HP using the engineered strains. (D) Relative activity of MatB of the engineered strains. (E) Relative activity of MCR of the engineered strains.

mutant N940V/K1106W/S1114R improved the catalytic efficiency by 14.2-fold over the wild-type.⁷ Moreover, the enzyme activity increased when the N-terminal and C-terminal regions of MCR were separated by fusing a flexible linker between the two enzymatic units.⁴⁰ Hence, to enhance the production of 3HP, the MCR mutant N940V/K1106W/S1114R was employed, and the separation of N-terminal and C-terminal regions of MCR by a linker (GGGS) was attempted in this study. As depicted in Fig. 4B, it was found that these two proteins levels in crude cell extract were different, with varying cloning sites in the plasmid pRSFDuet-1. For *RpMatB* corresponding to 54 kDa, the strain SGN73 cloning the *RpMatB* encoding gene in the second cloning site of the vector outperformed the strain SGN74 carrying the *RpMatB* encoding gene in the first cloning site. For MCR corresponding to 132 kDa, the linker between the C-terminal domain and N-terminal domain did not influence the protein expression (SGN74 and SGN75). However, the MCR protein level dramatically decreased when the gene was cloned in the upstream site of the plasmid. For multi-gene clusters, the upstream genes usually have higher expression levels than the downstream genes.⁴² However, our results were an exceptional case, which were also observed in other studies.⁴³

The corresponding results of the *MatB* and MCR activities of the crude extract are in good agreement with above proteins level assays. In detail, the strain SGN73 showed the highest *MatB* activity, which was about 3 times higher than that of strains SGN74 and SGN75 (Fig. 4D). Also, the strain exhibited the maximum MCR activity when MCR with a linker encoding gene was inserted into the second cloning site of the vector (Fig. 4E). Under shaking flask conditions (Fig. 4C), the strain SGN74 was the most productive, reaching an observed titer of $0.27 \pm 0.03 \text{ g L}^{-1}$ 3-HP when the *RpMatB* encoding gene was inserted into the first cloning site of pRSFDuet-1 and the linker existed between C-terminal domain and N-terminal domain of MCR. Collectively, all these results indicate that the 3-HP synthetic reaction from malonyl-CoA catalyzed by MCR is the rate-limiting step for the whole 3-HP synthetic pathway. Compared with the strain SGN75, the production of 3-HP by the strain SGN74 increased 1-fold, suggesting the separation of the C-terminal domain and N-terminal domain of MCR indeed improved the enzymatic activity by facilitating the entrance of the substrate malonyl-CoA into the C-terminal domain active site.⁴⁰ Our findings prove that the adjustment of the protein expression level and balance of enzyme activities are essential in the multistep pathway to improve production. Some recent studies also focused on balancing the pathway enzymes.^{44–47} For instance, to balance the enzymatic activities of glycerol dehydratase (GDHt) and aldehyde dehydrogenase (ALDH), varying-strength promoters and bicistronic ribosome binding sites (RBSs) were attempted. As a result, the accumulation of intermediate 3-hydroxypropionaldehyde (3-HPA) was avoided and the production of 3-HP improved.⁴⁸ In addition, the production of 3-HP by the recombinant strain is highly dependent on the expression level of MCR-N and MCR-C.⁷

Lower expression levels of pathway genes and the use of low-copy-number plasmid positively affect the production of 3-HP.⁸

Since *E. coli* host cells can biosynthesize malonyl-CoA from glucose, it is possible that 3-HP was produced using this portion of malonyl-CoA. Thus, the ability of cells only harboring MCR to synthesize 3-HP from glucose was investigated. As shown in Fig. 4C, no 3-HP was detected when the cells only expressed MCR. In contrast, a considerable yield of 3-HP was observed in the engineered strain harboring the whole metabolite pathway from malonate, including malonate transporter, *MatB* and MCR. Thus, these results suggest that the total production of 3-HP originates from the additional added malonate instead of glucose.

3.4 Optimization of fermentation conditions

Fermentation conditions are of great importance because they play an important role in the formation and yield of the target product.⁴⁹ Thus, optimization of the fermentation conditions for engineered strains is a good way to improve product quality and quantity. The one-factor-at-a-time method is a closed-ended system for fermentation processes. Based on the classical method of changing one independent variable while fixing all others,^{50,51} this method can be used to optimize medium components as well as process conditions. Herein, the three most important factors, organic nitrogen source, induction temperature and inducer concentration were optimized to enhance the production of 3-HP using the strain SGN74.

3.4.1 Effect of organic nitrogen source on 3-HP production.

The nitrogen source in the medium plays a crucial role in enhancing the production of the desired product.⁵² Thus, to investigate the effect of the organic nitrogen source on 3-HP production, four different organic nitrogen sources were assessed at the 20 °C, with the concentration of IPTG and arabinose of 0.5 mM and 0.2%, respectively (Fig. 5A). Among the organic nitrogen supplements tested, the beef extract (Sinopharm Chemical Reagent Co., Ltd, China) permitted a significantly higher 3-HP production than the other organic nitrogen sources. The highest concentration of 3-HP was $0.37 \pm 0.05 \text{ g L}^{-1}$, which was about 4 times the lowest value observed. Similarly, the cell density reached the maximum when the beef extract (Sinopharm Chemical Reagent Co., Ltd, China) was used as the organic nitrogen source in the fermentation medium, suggesting that this nitrogen source enhanced the accumulation of 3-HP by accelerating cell growth.

3.4.2 Effect of induction temperature on 3-HP production.

Low induction temperatures can increase the amount of active recombinant enzymes because low temperatures reduce the inclusion bodies in engineered *E. coli*.⁵³ However, successful control of the cultivation temperature has to balance cell growth, enzyme expression and product formation.⁵³ Hence, in this study, to increase 3-HP production, the different induction temperatures of 16 °C, 20 °C, 30 °C, 34 °C and 37 °C were investigated. As shown in Fig. 5B, the maximum 3-HP production was obtained at 30 °C, at $0.56 \pm 0.06 \text{ g L}^{-1}$, which was about 1.4 times, 1.1 times and 1.4 times greater than that observed at 20 °C ($0.39 \pm 0.03 \text{ g L}^{-1}$), 34 °C ($0.49 \pm 0.04 \text{ g L}^{-1}$)

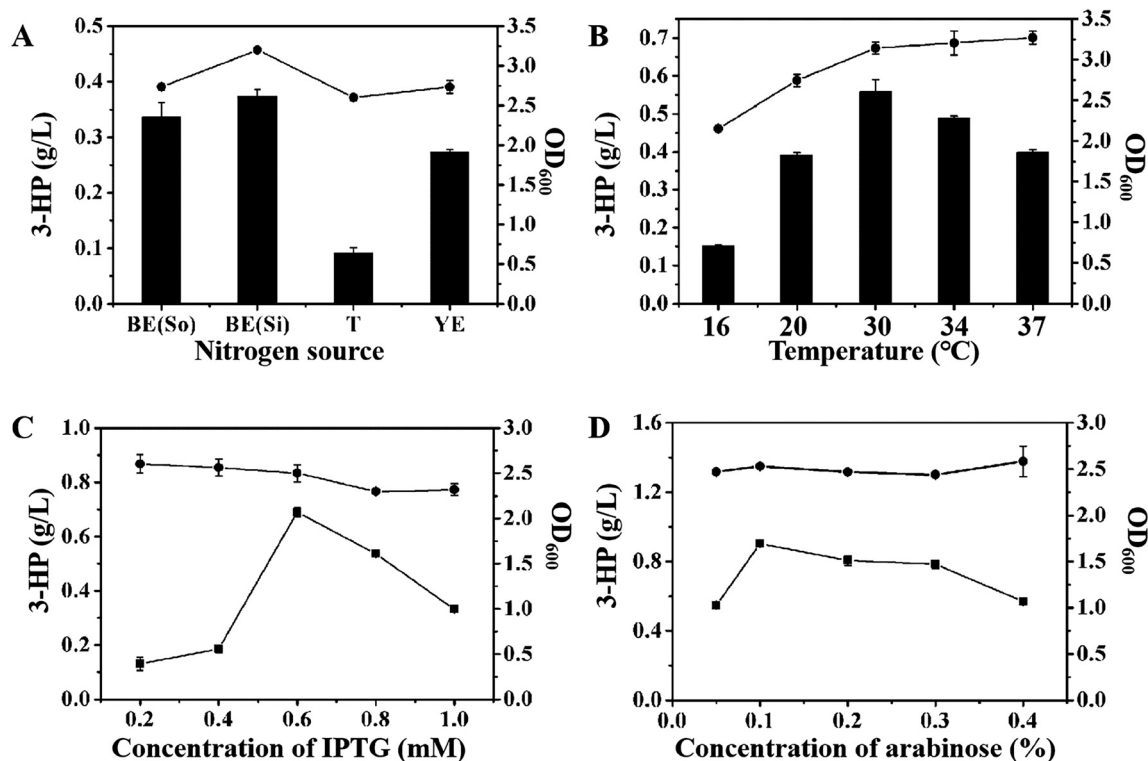


Fig. 5 Effects of fermentation source and culture conditions on 3-HP production by SGN74. (A) Effect of nitrogen source on 3-HP production: BE (So), beef extract from Solarbio; BE(Si), beef extract from Sinopharm; T, tryptone; and YE, yeast extract. (B) Effect of temperature on 3-HP production. (C) Effect of concentration of inducer IPTG on 3-HP production. (D) Effect of the concentration of arabinose on 3-HP production. Black line of filled circles, OD₆₀₀ value of strain SGN74. Black columns and black line of filled squares, 3-HP production under different fermentation conditions.

and 37 °C ($0.40 \pm 0.02 \text{ g L}^{-1}$), respectively. Hence, the optimum induction temperature for 3-HP production was 30 °C.

3.4.3 Effect of inducer concentration on 3-HP production.

In general, exogenous gene expression gives rise to a metabolic burden on cells, which can lead to reduced cell yields, growth rates, plasmid stability and product yield.^{54,55} Considering all the above factors, various IPTG and arabinose concentrations ranging from 0.2 mM to 1 mM and 0.05% to 0.4%, respectively, were tested to optimize the inducer concentration at the above-optimized temperature of 30 °C. As shown in Fig. S2,† obvious increased MCR and MatB levels were observed with an increase in the concentration of IPTG from 0.2 to 0.6. However, the amounts of expressed proteins decreased with a further increase in the concentration of IPTG. Based on the data shown in Fig. 5C and D, the yield of 3-HP reached a maximum of $0.90 \pm 0.07 \text{ g L}^{-1}$ when the concentrations of IPTG and arabinose were 0.6 mM and 0.1%, respectively. These results for 3-HP production are consistent with that from the SDS-PAGE analysis, indicating that inducers affect the synthesis of products by controlling the protein expression level. Moreover, the amounts of inducers have little effect on cell growth.

3.4.4 Effect of liquid volume on 3-HP production.

Suitable dissolved oxygen is a key factor in maintaining respiratory metabolism and product synthesis in aerobic microorganisms, and the amount of oxygen required by microorganisms varies

from strain to strain. Thus, to determine the optimal oxygen demand, cells were cultured in different liquid volumes. It can be seen from Fig. 5E that the dissolved oxygen has a significant effect on the growth of recombinant *E. coli* and the production of 3-HP. As the amount of liquid increased, the concentration of bacteria and 3-HP increased, and when the liquid volume reached 50 mL, the cell density of the cells and 3-HP production reached a maximum of 2.43 ± 0.22 and $1.01 \pm 0.03 \text{ g L}^{-1}$, respectively. Subsequently, the cell density and 3-HP titer began to decrease with a further increase in the liquid volume.

3.4.5 Effect of induction opportunity on 3-HP production.

The induction opportunity is an important factor influencing cell density and protein expression.⁵⁶ If the induction opportunity is too early, the expression of foreign proteins influences the physiological state of the cells, which is harmful to the growth of engineered bacteria and protein expression. If the induction opportunity is too late, the bacteria are aging, the nutrients in the medium are scarce, and the metabolic by-products increase, which are not conducive to protein expression. The results of the cell growth and 3-HP production by different induction opportunities are shown in Fig. 5F. When the inducers were added to the medium at the OD₆₀₀ of 0.6, the 3-HP production reached the maximum, suggesting that the optimum induction opportunity for 3-HP production was 0.6.

3.4.6 Effect of induction time on 3-HP production. *E. coli* cytoplasm has various proteolytic enzymes. Exogenous proteins are easily degraded by enzymes in the cytoplasm. Hence, the induction time is directly related to 3-HP production, fermentation cycle and cost. As shown in Fig. 5G, 3-HP production reached the highest level when the induction time was 16 h. After that, the output remained stable. Hence, the optimum induction time for 3-HP production was 16 h.

Based on the above data, the most suitable culture conditions for 3-HP production using the engineered strain SGN74 were 30 °C for 16 h, 0.6 mM IPTG, 0.1% arabinose, induction opportunity at OD₆₀₀ of 0.6 and 50 mL fermentation medium with beef extract (Sinopharm) as the organic nitrogen source.

3.5 Improvement of NADPH supply for enhancing 3-HP production

The N-terminal and the C-terminal regions of MCR are functionally distinct, which catalyze the two-step reduction of malonyl-CoA to 3-hydroxypropionate (3HP). Each step consumes 1 mol NADPH, and accordingly, the production of 1 mol of 3-HP requires 2 mol of NADPH (Fig. 1). Thus, the NADPH supply is an important factor influencing the efficiency of the 3-HP biosynthetic pathway.

In *E. coli*, the three major sources of NADPH regeneration are the pentose phosphate pathway (PPP), tricarboxylic acid cycle (TCA) and membrane-bound transhydrogenase (PntAB).⁵⁷ PntAB is a membrane-bound proton translocating transhydrogenase, which transfers a hydride from NADH to NADP⁺ with the concurrent production of NADPH and NAD⁺, powered by the proton motive force.⁵⁸ Thus, to recycle NAD⁺ for continuous transhydrogenation, NAD⁺ needs to be converted to NADP⁺ (Fig. 1).

In this work, to enhance the NADPH supply in the cells, NAD kinase (YfjB), which catalyzes the phosphorylation of NAD⁺ to NADP⁺, was over-expressed together with transhydrogenase in the engineered strain SGN74. Under shaking flask conditions, the strain SGN78 with the overexpression of PntAB and YfjB could accumulate 1.20 ± 0.08 g L⁻¹ 3-HP, which resulted in about 33.33% increase of 3-HP titer produced by the control strain SGN74. NADPH is tightly regulated in the cell. Studies have been conducted to manipulate the levels of NADPH in the cytosol. The results showed that the strain SGN78 produced 0.22 ± 0.02 nmol mL⁻¹ NADPH, 31.14% higher than that of strain SGN74 (0.17 ± 0.02 nmol mL⁻¹), indicating that PntAB and YfjB over-expression improved the NADPH production, which in turn promoted the biosynthesis of 3-HP. This result demonstrates that the co-expression of PntAB and YfjB can lead to a synergistic effect on increasing the NADPH supply and improving 3-HP production.

Table 2 shows recent studies on the bioproduction of 3-HP through the malonyl-CoA-mediated biosynthetic pathway from different feedstocks. For small-scale fermentation, the 3-HP titer of strain SGN78 in the present study was much higher than that of most engineered strains, demonstrating the efficient production of 3-HP from malonate. *E. coli* recombinant strains using glucose or fatty acids as substrates showed slightly higher titers than that of strain SGN78, indicating that the present

Table 2 Production of 3-HP through malonyl-CoA-mediated biosynthetic pathway from different feedstocks

Feedstock	Organism	Titer of shake-flask (g L ⁻¹)	Ref.
Glucose	<i>Saccharomyces cerevisiae</i>	0.46	59
Glucose	<i>Klebsiella pneumoniae</i>	1.8	60
CO ₂	<i>Synechocystis sp. PCC6803</i>	0.83	16
Glucose	<i>E. coli</i>	3.72 ± 0.01	7
Glucose	<i>Saccharomyces cerevisiae</i>	0.477 ± 0.001	10
Methanol	<i>Methylobacterium extorquens</i>	0.0698	17
Glucose	<i>Schizosaccharomyces pombe</i>	1.0	11
Fatty acids	<i>E. coli</i>	5.38 ± 0.53	8
Malonate	<i>E. coli</i>	1.20 ± 0.08	This study

work has great potential. Thus, to further improve the 3-HP production, a series of studies will be conducted in the following study, including optimization of promoter and RBSs, genome integration of function genes, and large-scale fermentation.

4. Conclusions

In this study, we successfully constructed a novel malonyl-CoA-mediated biosynthetic pathway in an engineered *E. coli* strain, which could produce high levels of 3-HP directly from malonate. Using a multi-step metabolic engineering strategy designed to increase the precursor and NADPH cofactor supplies for 3-HP production, the final engineered strain produced 1.20 ± 0.08 g L⁻¹ of 3-HP in flask culture. Thus, our work thus demonstrated the production of 3-HP in *E. coli* with the shortest route for the biosynthesis of 3-HP, which involved only three steps. Also, it opens new possibilities to produce other malonyl-CoA-based valuable chemicals directly from malonate in *E. coli*.

Conflicts of interest

There are no conflicts of interest to declare.

Acknowledgements

This work was supported by the National Natural Science Foundation of China (Grant No. 21572242), the Talents of High Level Scientific Research Foundation (Grant No. 6631113326; 6651119011) of Qingdao Agricultural University. Many thanks to Caroline Stone Harwood for deep discussion and helpful suggestions.

References

- 1 T. Werpy and G. Petersen, Energy efficiency and renewable energy, US Department of Energy, Washington D.C, 2004.

- 2 F. de Foucheour, A. K. Sanchez-Castaneda, C. Saulou-Berion and H. E. Spinnler, *Biotechnol. Adv.*, 2018, **36**, 1207–1222.
- 3 C. Della Pina, E. Falletta and M. Rossi, *Green Chem.*, 2011, **13**, 1624–1632.
- 4 F. Long and M. Purchase, *J. Am. Chem. Soc.*, 1950, **72**, 3267–3273.
- 5 A. Behr, A. Botulinski, F.-J. Carduck and M. Schneider, *US Patent*, 5321156, 1994.
- 6 R. Y. Ji, Y. Ding, T. Q. Shi, L. Lin, H. Huang, Z. Gao and X. J. Ji, *Front. Microbiol.*, 2018, **9**, 2185.
- 7 C. S. Liu, Y. M. Ding, R. B. Zhang, H. Z. Liu, M. Xian and G. Zhao, *Metab. Eng.*, 2016, **34**, 104–111.
- 8 B. Liu, S. Xiang, G. Zhao, B. Wang, Y. Ma, W. Liu and Y. Tao, *Metab. Eng.*, 2019, **51**, 121–130.
- 9 H. Luo, D. Zhou, X. Liu, Z. Nie, D. L. Quiroga-Sanchez and Y. Chang, *PLoS One*, 2016, **11**, e0156286.
- 10 X. X. Chen, X. Y. Yang, Y. Shen, J. Hou and X. M. Bao, *ACS Synth. Biol.*, 2017, **6**, 905–912.
- 11 S. Takayama, A. Ozaki, R. Konishi, C. Otomo, M. Kishida, Y. Hirata, T. Matsumoto, T. Tanaka and A. Kondo, *Microb. Cell Fact.*, 2018, **17**, 176.
- 12 Y. Li, X. Wang, X. Z. Ge and P. F. Tian, *Sci. Rep.*, 2016, 26932.
- 13 Y. N. Huang, Z. M. Li and Q. Ye, *Appl. Biochem. Biotechnol.*, 2016, **178**, 1129–1140.
- 14 Z. Chen, J. H. Huang, Y. Wu, W. J. Wu, Y. Zhang and D. H. Liu, *Metab. Eng.*, 2017, **39**, 151–158.
- 15 E. I. Lan, D. S. Chuang, C. R. Shen, A. M. Lee, S. Y. Ro and J. C. Liao, *Metab. Eng.*, 2015, **31**, 163–170.
- 16 Y. Wang, T. Sun, X. Gao, M. Shi, L. Wu, L. Chen and W. Zhang, *Metab. Eng.*, 2016, **34**, 60–70.
- 17 Y. M. Yang, W. J. Chen, J. Yang, Y. M. Zhou, B. Hu, M. Zhang, L. P. Zhu, G. Y. Wang and S. Yang, *Microb. Cell Fact.*, 2017, **16**, 179.
- 18 Y. A. Chan, A. M. Podevels, B. M. Kevany and M. G. Thomas, *Nat. Prod. Rep.*, 2009, **26**, 90–114.
- 19 T. Liu, H. Vora and C. Khosla, *Metab. Eng.*, 2010, **12**, 378–386.
- 20 C. S. Liu, Y. M. Ding, M. Xian, M. Liu, H. Z. Liu, Q. J. Ma and G. Zhao, *Crit. Rev. Biotechnol.*, 2017, **37**, 933–941.
- 21 A. M. Gulick, *ACS Chem. Biol.*, 2009, **4**, 811–827.
- 22 Y. S. Kim and S. K. Bang, *J. Biol. Chem.*, 1985, **260**, 5098–5104.
- 23 C. E. Bowman, S. Rodriguez, E. S. S. Alpergin, M. G. Acoba, L. Zhao, T. Hartung, S. M. Claypool, P. A. Watkins and M. J. Wolfgang, *Cell Chem. Biol.*, 2017, **24**, 673–684.
- 24 Y. S. Kim and S. W. Kang, *Biochem. J.*, 1994, **297**(Pt 2), 327–333.
- 25 J. H. An and Y. S. Kim, *Eur. J. Biochem.*, 1998, **257**, 395–402.
- 26 A. J. Hughes and A. Keatinge-Clay, *Chem. Biol.*, 2011, **18**, 165–176.
- 27 H. A. Crosby, K. C. Rank, I. Rayment and J. C. Escalante-Semerena, *Appl. Environ. Microbiol.*, 2012, **78**, 6619–6629.
- 28 R. Vancraenenbroeck, S. Kunzelmann and M. R. Webb, *PLoS One*, 2017, **12**, e0179547.
- 29 Y. S. Kim and H. Z. Chae, *Biochem. J.*, 1991, **273**(Pt 3), 511–516.
- 30 Y. S. Kim, *Clin. Infect. Dis.*, 2002, **35**, 443–451.
- 31 Y. C. Wang, H. Chen and O. Yu, *Appl. Microbiol. Biotechnol.*, 2014, **98**, 5435–5447.
- 32 S. R. Park, M. S. Ahn, A. R. Han, J. W. Park and Y. J. Yoon, *J. Microbiol. Biotechnol.*, 2011, **21**, 1143–1146.
- 33 I. A. Suvorova, D. A. Ravcheev and M. S. Gelfand, *J. Bacteriol.*, 2012, **194**, 3234–3240.
- 34 J. A. Forward, M. C. Behrendt, N. R. Wyborn, R. Cross and D. J. Kelly, *J. Bacteriol.*, 1997, **179**, 5482–5493.
- 35 A. M. Chen, Y. B. Wang, S. Jie, A. Y. Yu, L. Luo, G. Q. Yu, J. B. Zhu and Y. Z. Wang, *Res. Microbiol.*, 2010, **161**, 556–564.
- 36 C. Mulligan, M. Fischer and G. H. Thomas, *FEMS Microbiol. Rev.*, 2011, **35**, 68–86.
- 37 C. Mulligan, E. R. Geertsma, E. Severi, D. J. Kelly, B. Poolman and G. H. Thomas, *Proc. Natl. Acad. Sci. U. S. A.*, 2009, **106**, 1778–1783.
- 38 L. P. Feng, J. W. Zhu, H. T. Chang, X. P. Gao, C. Gao, X. F. Wei, F. Y. Yuan and W. C. Bei, *Sci. Rep.*, 2016, **6**, 21241.
- 39 J. H. An, G. Y. Lee, J. Jin-Won, L. Weontae and Y. S. Kim, *Biochem. J.*, 1999, **344**, 159–166.
- 40 C. S. Liu, Q. Wang, M. Xian, Y. M. Ding and G. Zhao, *PLoS One*, 2013, **8**, e75554.
- 41 H. Chen, H. U. Kim, H. Weng and J. Browse, *Plant Cell*, 2011, **23**, 2247–2262.
- 42 H. Chen, R. Huang and Y. H. P. Zhang, *Appl. Microbiol. Biotechnol.*, 2017, **101**, 4481–4493.
- 43 Y. Zhu, H. Li, P. Liu, J. Yang, X. Zhang and Y. Sun, *J. Ind. Microbiol. Biotechnol.*, 2015, **42**, 661–669.
- 44 J. A. Houwman, T. Knaus, M. Costa and F. G. Mutti, *Green Chem.*, 2019, **21**, 3846–3857.
- 45 N. Oberleitner, C. Peters, J. Muschiol, M. Kadow, S. Saß, T. Bayer, P. Schaaf, N. Iqbal, F. Rudroff and M. D. Mihovilovic, *ChemCatChem*, 2013, **5**, 3524–3528.
- 46 S. Wu and Z. Li, *ChemCatChem*, 2018, **10**, 2164–2178.
- 47 S. Liu, X. Zhang, F. Liu, M. Xu, T. Yang, M. Long, J. Zhou, T. Osire, S. Yang and Z. Rao, *ACS Synth. Biol.*, 2019, **8**, 734–743.
- 48 M. Sankaranarayanan, A. Somasundar, E. Seol, A. S. Chauhan, S. Kwon, G. Y. Jung and S. Park, *J. Biotechnol.*, 2017, **259**, 140–147.
- 49 F. R. Schmidt, *Appl. Microbiol. Biotechnol.*, 2005, **68**, 425–435.
- 50 M. Zafferahamad, P. S. Javed and M. Ali, *Res. J. Microbiol.*, 2010, **5**, 1165–1169.
- 51 Y. V. Alexeeva, E. P. Ivanova, I. Y. Bakunina, T. N. Zvaygintseva and V. V. Mikhailov, *Lett. Appl. Microbiol.*, 2002, **35**, 343–346.
- 52 M. A. J. Torija, G. Beltran, M. Novo, M. Poblet, N. Rozès, J. M. Guillamón and A. Mas, *Food Microbiol.*, 2003, **20**, 255–258.

- 53 N. S. de Groot and S. Ventura, *FEBS Lett.*, 2006, **580**, 6471–6476.
- 54 W. E. Bentley, N. Mirjalili, D. C. Andersen, R. H. Davis and D. S. Kompala, *Biotechnol. Bioeng.*, 2009, **102**, 1284–1297; discussion 1283.
- 55 B. R. Glick, *Biotechnol. Adv.*, 1995, **13**, 247–261.
- 56 Y. M. Jiang, W. Y. Tong and D. Z. Wei, *Biotechnol. Prog.*, 2007, **23**, 1031–1037.
- 57 U. Sauer, F. Canonaco, S. Heri, A. Perrenoud and E. Fischer, *J. Biol. Chem.*, 2004, **279**, 6613–6619.
- 58 D. M. Clarke and P. D. Bragg, *Eur. J. Biochem.*, 1985, **149**, 517–523.
- 59 Y. Chen, J. C. Bao, I. K. Kim, V. Siewers and J. Nielsen, *Metab. Eng.*, 2014, **22**, 104–109.
- 60 Z. Cheng, J. Jiang, H. Wu, Z. Li and Q. Ye, *Bioresour. Technol.*, 2016, **200**, 897–904.